The SEMATECH Berkeley MET pushing EUV development beyond 22-nm half pitch

Patrick Naulleau,[1] Christopher N. Anderson,[1] Lorie-Mae Baclea-an,[1] David Chan,[3] Paul Denham,[1] Simi George,[1] Kenneth A. Goldberg,[1] Brian Hoef,[1] Gideon Jones,[1] Chawon Koh,[3] Bruno La Fontaine,[4] Brittany McClinton,[2] Ryan Miyakawa,[2] Warren Montgomery,[3] Seno Rekawa,[1] and Tom Wallow[4]

[1]Center for X-Ray Optics, Lawrence Berkeley National Laboratory, Berkeley, CA 94720
[2]University of California, Berkeley, CA 94720
[3]SEMATECH, Albany, NY 12203
[4]Global Foundries, Sunnyvale, CA 94088

ABSTRACT

Microfield exposure tools (METs) play a crucial role in the development of extreme ultraviolet (EUV) resists and masks. One of these tools is the SEMATECH Berkeley 0.3 numerical aperture (NA) MET. Using conventional illumination this tool is limited to approximately 22-nm half pitch resolution. However, resolution enhancement techniques have been used to push the patterning capabilities of this tool to half pitches of 18 nm and below. This resolution was achieved in a new imageable hardmask which also supports contact printing down to 22 nm with conventional illumination. Along with resolution, line-edge roughness is another crucial hurdle facing EUV resists. Much of the resist LER, however, can be attributed to the mask. We have shown that intenssionally aggressive mask cleaning on an older generation mask causes correlated LER in photoresist to increase from 3.4 nm to 4.0 nm. We have also shown that new generation EUV masks (100 pm of substrate roughness) can achieve correlated LER values of 1.1 nm, a 3× improvement over the correlated LER of older generation EUV masks (230 pm of substrate roughness). Finally, a 0.5-NA MET has been proposed that will address the needs of EUV development at the 16-nm node and beyond. The tool will support an ultimate resolution of 8 nm half-pitch and generalized printing using conventional illumination down to 12 nm half pitch.

Keywords: extreme ultraviolet, lithography, photoresist, mask roughness, mask cleaning, nanolithography

1. INTRODUCTION

Microfield exposure tools (METs) [1-3] have and continue to play a dominant role in the development of extreme ultraviolet (EUV) resists and masks. One of these tools is the SEMATECH Berkeley 0.3 numerical aperture (NA) MET [1]. Using conventional illumination, this tool is limited to approximately 22-nm half pitch resolution. Here we describe and demonstrate resolution enhacement techniques capable of pushing the SEMATECH Berkeley MET (BMET) beyond this limit. We consider both a strictly illumination-based method as well as a system-based method which is functionally equivalent to using a chromeless phase shift mask yet requires only a simple binary amplitude mask.

We use the methods described above to demonstrate patterning at the sub-22-nm level and summarize the latest resist performance results, including resolution, line edge roughness (LER), and sensitivity. Noting that the high coherence required to implement the resolution enhancement methods also introduces significant LER, we provide an update on mask contributions to LER exploring the effects of mask cleaning as well as the capabilities of the latest EUV masks.

2. BMET RESOLUTION ENHANCEMENT

With EUV resists having reached resolution levels of 20 nm [4], the modified illumination capabilities [5] of the BMET are crucial to further progress. Figure 1 shows the computed aerial image contrast for the BMET using its conventional annular 0.35-0.55 illumination as well as dipole illumination optimized for 18-nm half pitch. With conventional annular illumination, the contrast roll-off occurs at approximately 25-nm half pitch. In the dipole case, excellent performance is achieved in the 16-22-nm range, however, the dipole case suffers from forbidden pitches in the 25-nm to 50-nm CD

range. The ultimate capabilities of the dipole illumination are demonstrated experimentally in Fig. 2 which shows a zoomed out image of a series of equal line-space patterns ranging from 100 nm down to 12 nm. The forbidden pitches are clearly seen as well as the small CD cutoff. Note that bright areas in the image do not necessarily imply quality imaging but rather simply indicates the presence of the diffracted orders necessary to achieve printing; in practice, the actual printing performance will be limited by the resolution of the photoresist. Figure 3 shows a plot of the captured diffracted order intensity as a function of CD for the dipole illumination which is much more comparable to what is visualized in Fig. 2.

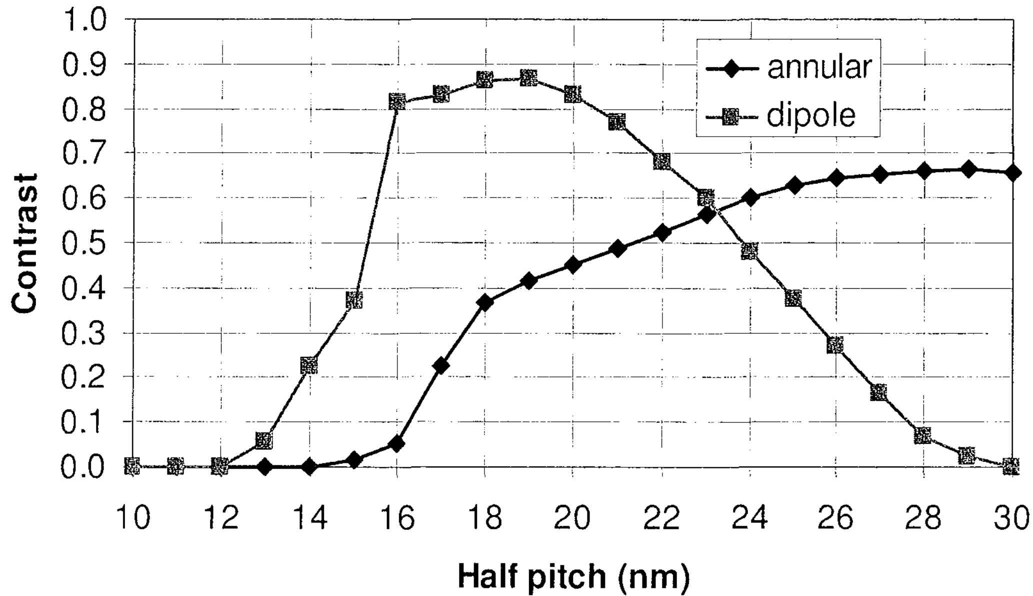

Fig. 1. Computed aerial image contrast for the BMET using its conventional annular 0.35-0.55 illumination as well as dipole illumination optimized for 18-nm half pitch.

Although the dipole setting addresses NA limitations, it does not help in overcoming any potential mask resolution limitations. Mask resolution limitations could be overcome through the use of chromeless phase shift mask technology which has the ability for pitch splitting. Fabricating a high quality chromeless phase shift mask for EUV, however, is certainly not a trivial task and in practice may be a greater limitation than the resolution on a conventional mask. Fundamentally, a chromeless phase shift mask enables pitch splitting by suppression of the zeroth diffracted order from the line-space pattern on the mask. This is achieved by having a perfect π phase shift between the line and the space while simultaneously having constant reflectivity from both the line and space. In such a case, the average field value (DC term) at the exit surface of the phase shift structure is zero and thus the zeroth diffracted order is suppressed. Should we be able to use some other mechanism to suppress the zeroth order, we would be able to achieve the identical pitch splitting characteristic. One possible way to achieve this is through spatial filtering at the Fourier plane of the mask pattern. Noting that the mask Fourier transform appears at the imaging optic pupil plane, the requisite spatial filtering could be achieved in that plane. Efficient spatial filtering requires simply that the separation of the orders of interest is large compared to the pupil fill. For feature sizes in the sub-20-nm range, this is readily achieved with σ values smaller than 0.1. Being equipped with lossless pupil fill control, such a σ is easily attained with the BMET. The next requirement for spatial filtering is the actual aperture needed to block the zeroth order. Noting, however, that the MET is a centrally obscured system, the required aperture is already built in and requires only that we steer the pupil fill to the center of the pupil such that it is completely blocked by the central obscuration. In this case the +/-1 diffracted orders

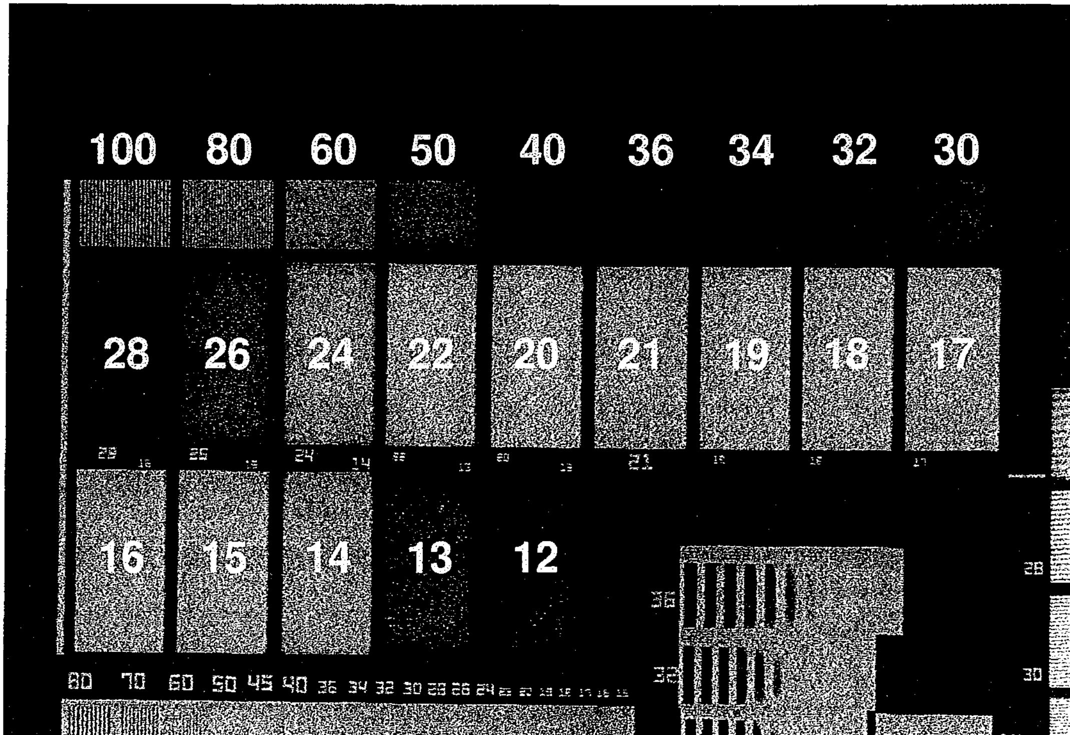

Fig. 2. Zoomed out image of a series of equal line-space patterns ranging from 100 nm down to 12 nm. The forbidden pitches are clearly seen as well as the small CD cutoff.

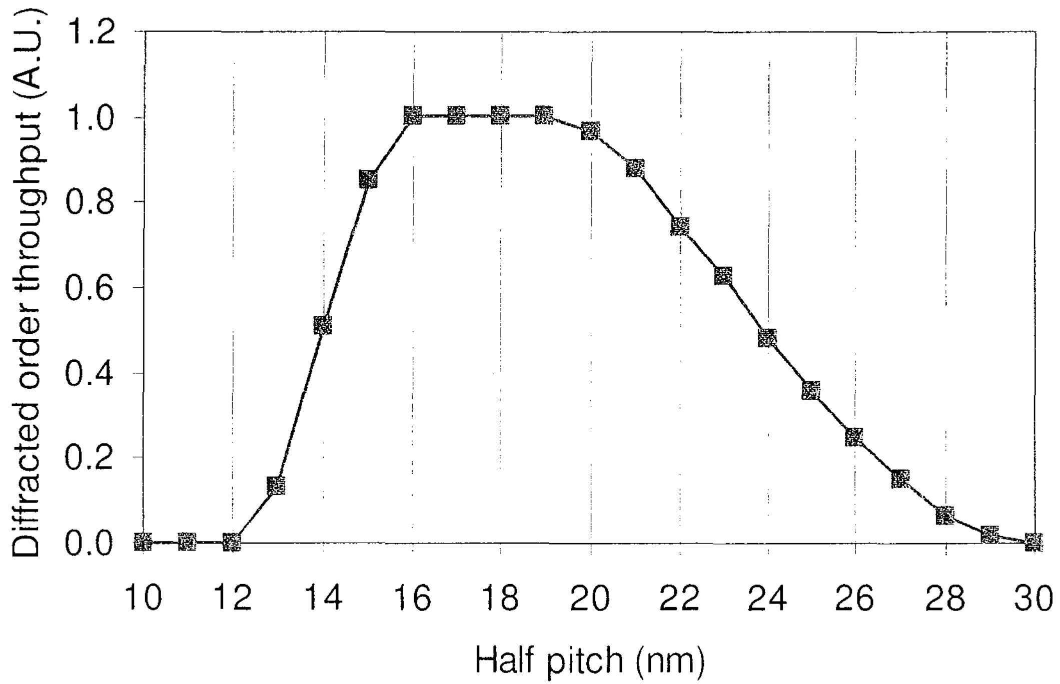

Fig. 3. Plot of captured diffracted order intensity as a function of CD for the dipole illumination. This data is directly comparable to the results visualized in Fig. 2.

will be captured by the clear aperture and the zeroth order blocked, providing a functional equivalent to the chromeless phase shift mask while using a conventional binary amplitude mask. We refer to this process as Pseudo Phase Shift Mask (Pseudo-PSM). Figure 4 shows a schematic of this process along with exposures of 45-nm lines and spaces using both conventional illumination and the Pseudo-PSM method which results in twice as many 22.5-nm lines and spaces. Note that the tone of the image also changes due to the complete removal of the DC term, even the clear areas. This is different than the behavior of a chromeless phase shift mask which only achieves DC suppression in the region of the lines themselves and not in large open areas.

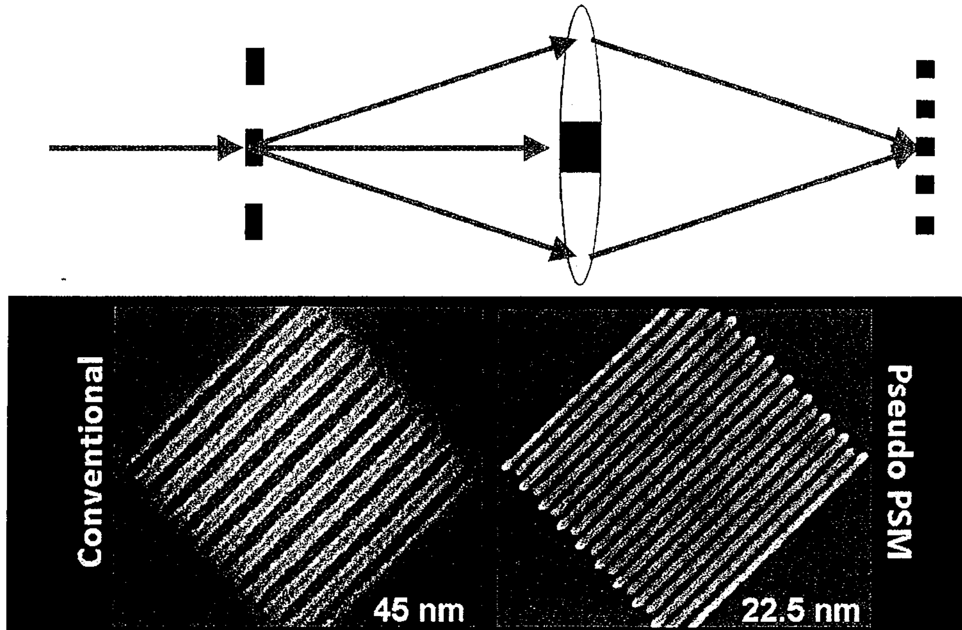

Fig. 4. Schematic of the pseudo-PSM process along with exposures of 45-nm lines and spaces using both conventional illumination and the Pseudo-PSM method which results in twice as many 22.5-nm lines and spaces.

3. RECENT RESIST TESTING RESULTS

Having demonstrated good 22-nm half pitch performance last year [4], the goal has been pushed to 20-nm half pitch and below. While the past year has brought significant improvement in the range of materials achieving 22-nm resolution as well as slight improvements in LER and sensitivity [6], conventional chemically amplified resist have shown minimal gains in the area of ultimate resolution. This fact is borne out in Fig. 5 comparing 20-nm and below printing results for the late 2008 champion resist (BBR-08b) to three of the highest performing resists developed over the past year. These results were obtained with the 18-nm optimized dipole setting described above. To demonstrate that the observed resolution is not mask induced, we also imaged the BBR-08b resist in the Pseudo-PSM configuration (Fig. 6).

Despite limited progress with conventional resists, strong gains have been made in the area of ultimate resolution with a directly imageable metal oxide hardmask. Figure 7 shows Pseudo-PSM printing results in such a material provided by Inpria [7]. Although improvements in contrast are still required, the striking improvement in ultimate resolution is clearly evident. The sizing dose in this material is approximately 40 mJ/cm^2 but significant improvements in speed are feasible. The sensitivity/resolution tradeoffs in this material are currently being explored. This same material also performs well in printing posts as demonstrated in Fig. 8 where the printing of 22-nm posts is demonstrated using conventional annular illumination.

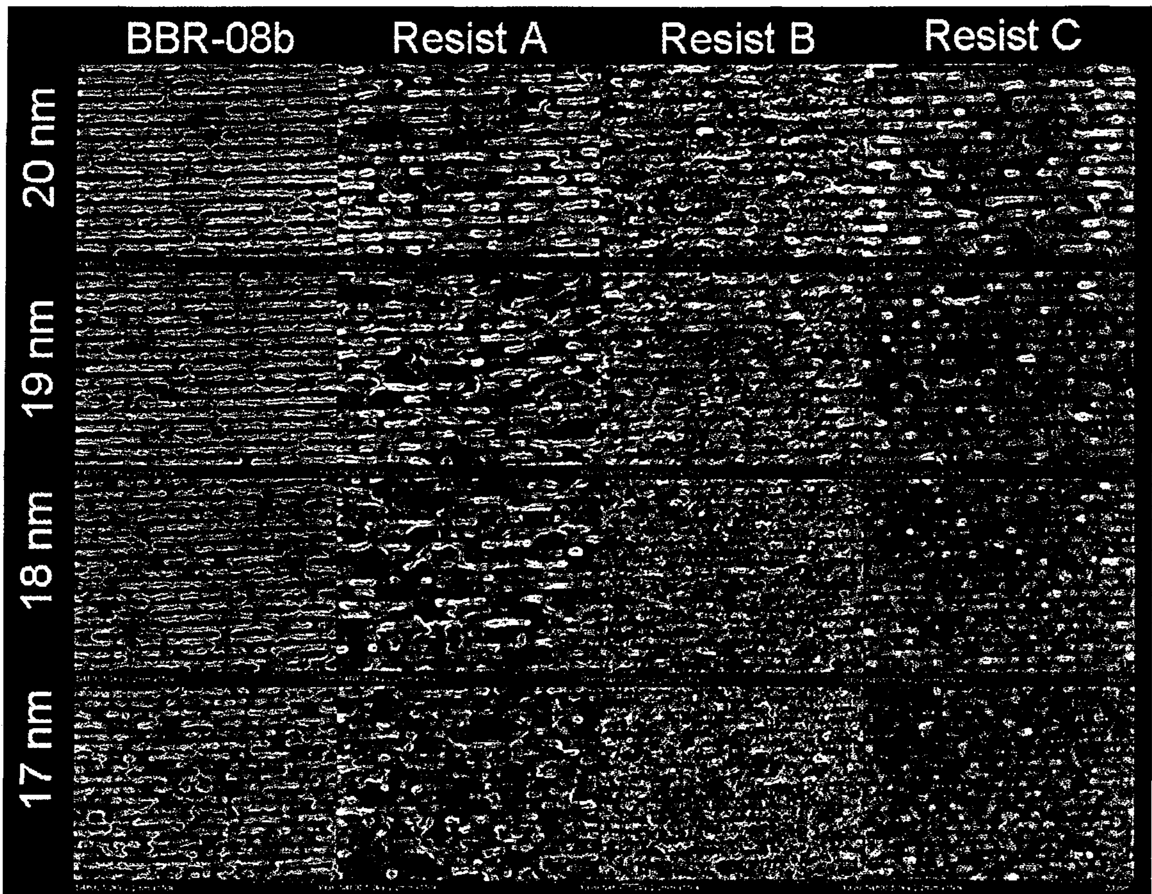

Fig. 5. Direct comparison the BBR-08b developed in late 2008 to three of the highest performing resists developed over the past year.

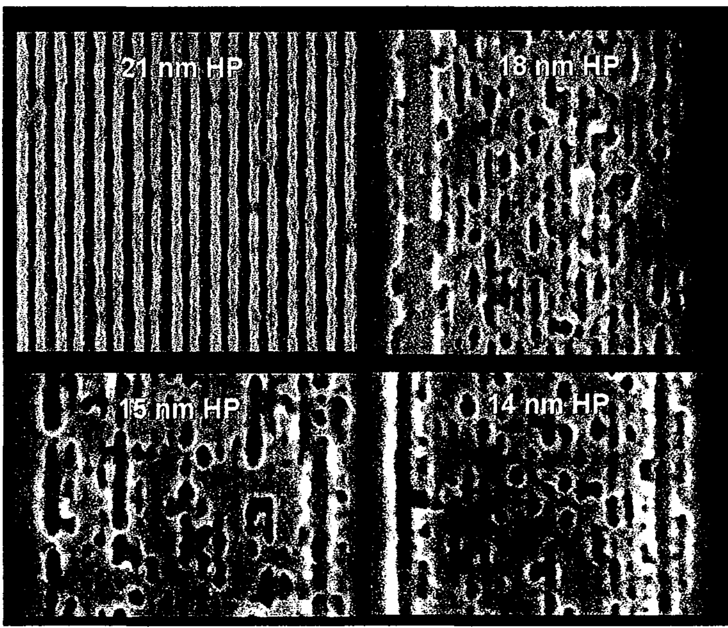

Fig. 6. Pseudo-PSM mode printing in BBR-08b demonstrating that we are not mask limited in terms of resolution.

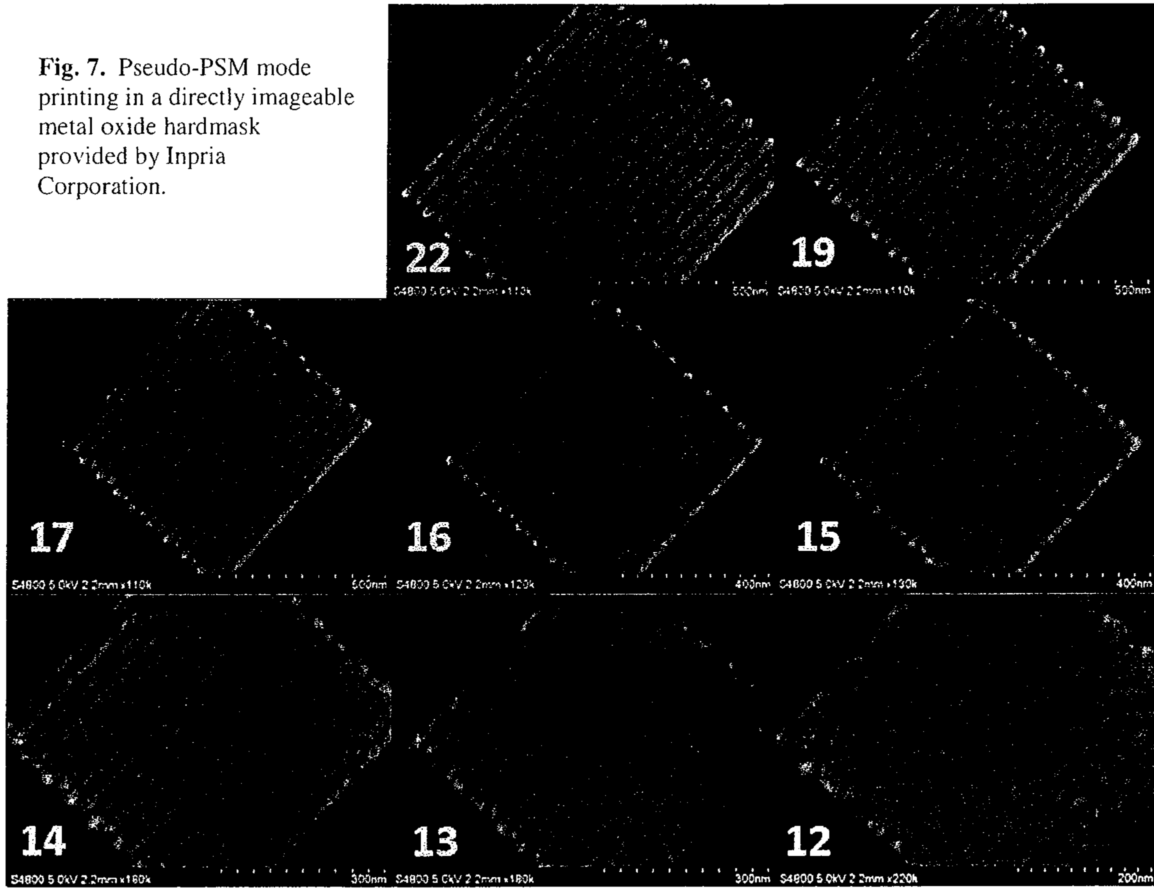

Fig. 7. Pseudo-PSM mode printing in a directly imageable metal oxide hardmask provided by Inpria Corporation.

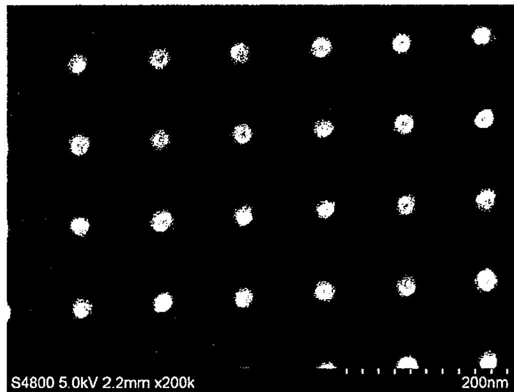

Fig. 8. 22-nm posts printed in the Inpria material using conventional annular illumination.

3. MASK CONTRIBUTIONS TO LER

Mask effects are now understood to be an important factor in image plane LER [8-12]. More recently, these effects have been systematically characterized using an exposure to exposure correlation method [13]. The results showed the mask-limited LER under $\sigma = 0.05$ illumination to be 3.4 nm. Modeling showed the majority of this roughness to originate from substrate-induced phase roughness. These results raised the associated question of capping layer roughness and the potential impact of mask cleaning on image plane LER. To address this concern, an intentionally aggressive cleaning

process was employed on our mask and the effect on LER characterized. Figure 9 shows a direct comparison of the correlated LER measurement at the exact same area on the mask before and after cleaning. The imaging conditions are $\sigma = 0.05$ and defocus = 100 nm. The correlated LER is seen to increase from 3.4 nm to 4.0 nm. Repeating this measurement for lower coherence annular illumination, we find an identical increase in correlated LER suggesting that the cleaning damage caused reflective variations across the mask as opposed to only phase variations. The results also show that the uncorrelated LER increased by approximately 1 nm suggesting a degradation in image log slope leading to increased LER from the resist.

It is important to note that the mask used in this test is now quite old and has significantly higher substrate roughness than currently achievable (230 pm versus approximately 100-150 pm). As shown in Fig. 10, performing a similar analysis on a new generation mask produces significantly lower correlated roughness. Again using $\sigma = 0.5$ and 100 nm defocus, on the new mask we find a correlated LER of only 1.1 nm. Further measurements varying illumination coherence and defocus are required in order to determine the primary source of remaining correlated LER (phase roughness or absorber LER).

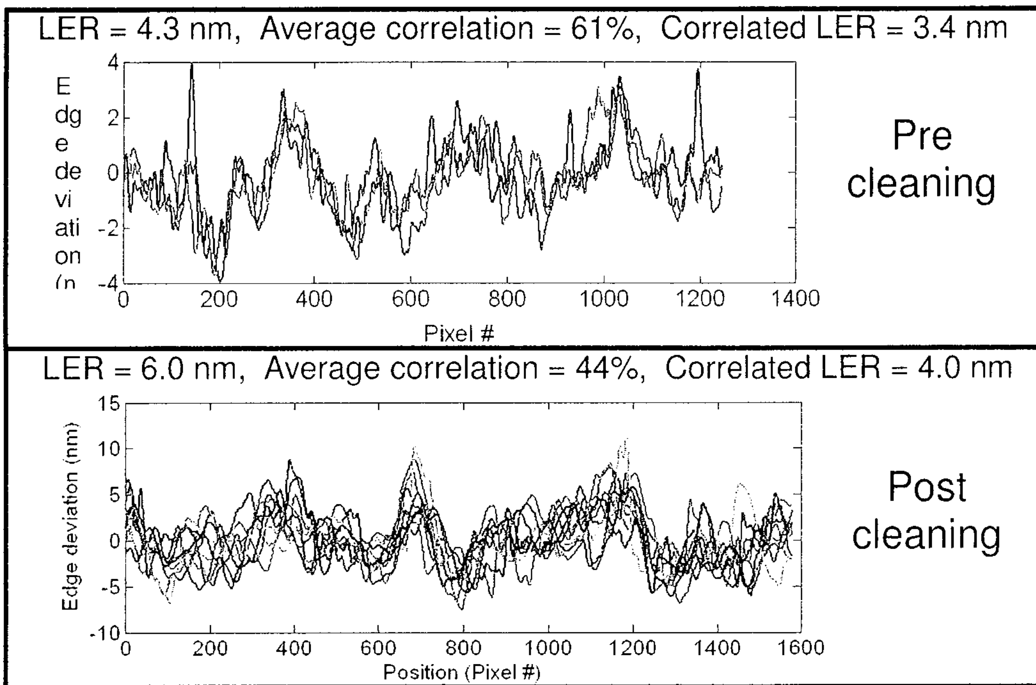

Fig. 9. Direct comparison of the correlated LER measurement at the exact same area on the mask increase is 0.6 nm and the uncorrelated LER increase is 1 nm.

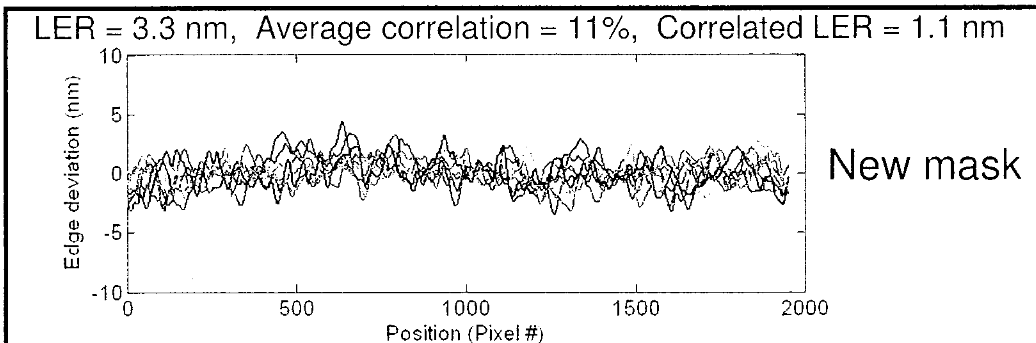

Fig. 10. Correlated LER measurement on new mask with $\sigma = 0.5$ and 100-nm defocus.

4. FUTURE PLANS

Although modified illumination can push the resolution of the 0.3 NA BMET down below 20 nm, the benefits are quite restrictive in terms of the required high coherence illumination conditions and pattern flexibility. These restrictions have significant impact on resist learning that can be done in the areas of iso-dense bias, through-pitch performance, contact printing, etc. The restrictions are even more important in the area of mask development significantly limiting learning in the areas of defect printability, optical proximity correction, mask architecture, etc. Clearly, more generalized EUV learning and development at the 16-nm node and below will require a higher NA system. To this end, SEMATECH has initiated a plan to implement a 0.5 NA microfield tool at the Advanced Light Source synchrotron facility. A diagram of proposed two mirror optical system [14] is shown in Fig. 11. The system has a magnification of 5, a field of view of 200×30 μm, and a mask angle of incidence of 6°. With modified illumination, the system has a resolution limit of 8 nm (Fig. 12), and with conventional illumination the system can easily resolve 12-nm features as depicted in Fig. 13.

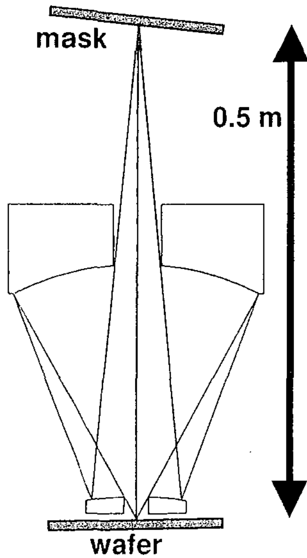

Fig. 11. Schematic of proposed 0.5-NA microfield lithography optic.

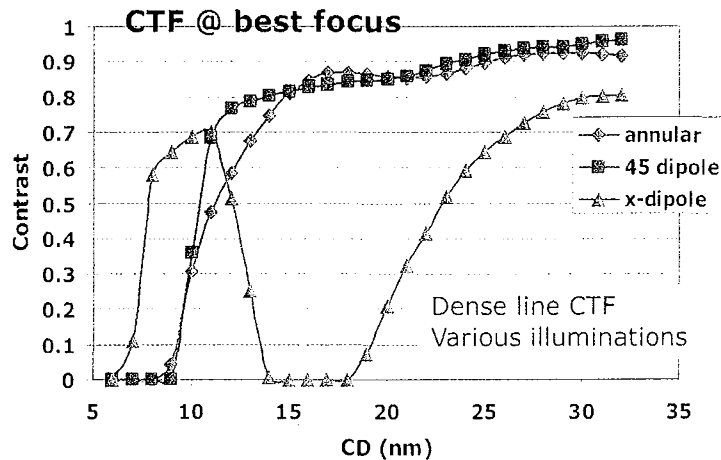

Fig. 12. Modeled performance of 0.5-NA system in imaging equal lines and spaces under three different illumination conditions.

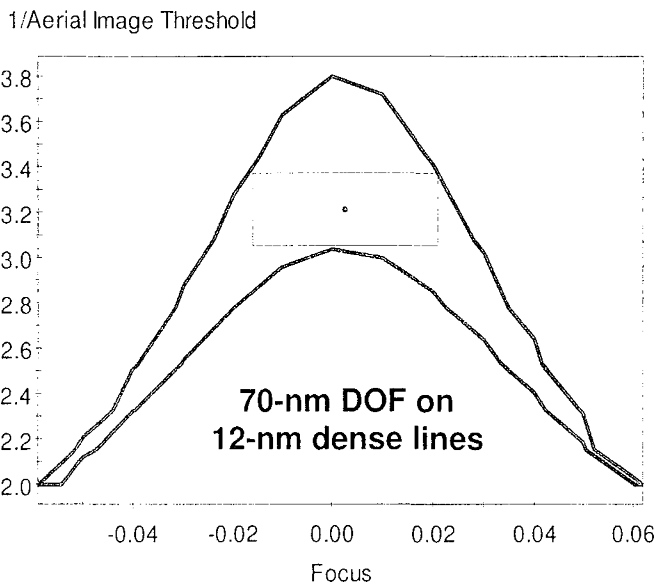

Fig. 13. Modeled process window performance of 0.5-NA system in imaging 12 nm equal lines and spaces using conventional annular illumination.

5. SUMMARY

As we enter the realm of sub-22-nm EUV development, resolution enhancing illumination capabilities are becoming increasingly important. Using a Pseudo-PSM method, the SEMATECH Berkeley MET has demonstrated resolution to 18-nm half pitch and below in an imageable spin-on hard mask.

Continued study of the mask effects on LER have revealed the potential negative impact of mask cleaning. Also, results have shown that new masks provide a significant improvement in correlated image-plane LER as compared to counterparts from three years ago. An improvement of approximately 3× was found.

Finally, to address the needs of EUV development at the 16-nm node and beyond, a new 0.5-NA microfield exposure tool has been proposed. This tool would support an ultimate resolution down to 8 nm and generalized printing using conventional illumination down to 12 nm.

The authors are greatly indebted to CXRO precision engineering including Kevin Bradley, Rene Delano, Drew Kemp, Jeff Gamsby, Bob Gunion, Farhad Salmassi, and Ron Tackaberry for building and maintaining the MET exposure tool. We also thank Jim Thackeray and Katherine Spear of Dow Chemical, Shinji Tarutani of Fujifilm, Yoshio Kawai of Shin Etsu, and Andrew Grenville and Jason Stowers of Inpria for excellent resist support. We thank Ted Liang, Robert Chen, and Guojing Zhang of Intel for mask support. Finally we thank Michael Goldstein of Intel and Russ Hudyma of Hyperion Development for support on the 0.5-NA optic design and modeling. This work was funded by SEMATECH and we thank Bryan Rice and Stefan Wurm for continued support of the SEMATECH MET exposure facility at the Advanced Light Source. The work was performed at Lawrence Berkeley National Laboratory's Advanced Light Source synchrotron facility which is supported by the DOE, Office of Science, Basic Energy Sciences. under Contract No. DE-AC02-05CH11231.

REFERENCES

1. P. Naulleau, *et al.*, "Status of EUV micro-exposure capabilities at the ALS using the 0.3-NA MET optic," Proc. SPIE **5374**, 881-891 (2004).
2. A. Brunton, *et al.*, "High-resolution EUV imaging tools for resist exposure and aerial image monitoring," Proc. SPIE **5751**, 78-89 (2005).
3. H. Oizumi, Y. Tanaka, I. Nishiyama, H. Kondo, K. Murakami, "Lithographic performance of high-numerical-aperture (NA=0.3) EUV small-field exposure tool (HINA)," Proc. SPIE **5751**, 102-109 (2005).
4. P. Naulleau, *et al*, "The SEMATECH Berkeley microfield exposure tool: learning at the 22-nm node and beyond." Proc. SPIE **7271**, 7271W (2009).
5. P. Naulleau, K. Goldberg, P. Batson, J. Bokor, P. Denham, and S. Rekawa, "A Fourier-synthesis custom-coherence illuminator for EUV microfield lithography," Appl. Opt. **42**, 820-826 (2003).
6. R. Caudillo, M. Chandhok, G. Kloster, E. Putna, Grant, U. Shah, T. Younkin, "Assessment of Resist Readiness for 22 hp EUV Lithography," 2009 International Symposium on Extreme Ultraviolet Lithography, Prague, Czech Republic, October 18- October 23, 2009, proceedings available from SEMATECH, Albany, NY (https://www.sematech.org/proceedings/order/8653.htm).
7. Material provided by A. Grenville and J. Stowers, Inpria Corporation, 2001 NW Monroe Ave Corvallis, OR 97330.
8. P. Naulleau and G. Gallatin, "The line-edge roughness transfer function and its application to determining mask effects in EUV resist characterization," Appl. Opt. **42**, 3390-3397 (2003).
9. N. Beaudry, T. Milster, "Effects of mask roughness and condenser scattering in EUVL systems," Proc. SPIE. **3676**, 653-662 (1999).
10. P. Naulleau, "The relevance of mask-roughness-induced printed line-edge roughness in recent and future EUV lithography tests," Appl. Opt. **43**, 4025-4032 (2004).
11. P. Naulleau, D. Niakoula, G. Zhang, "System-level line-edge roughness limits in extreme ultraviolet lithography," J. Vac. Sci. & Technol. B **26**, 1289-1293 (2008).
12. P. Naulleau and G. Gallatin, "Spatial scaling metrics of mask-induced line-edge roughness," J. Vac. Sci. & Technol. B **26**, 1903-1910 (2008).
13. P. Naulleau, "Correlation method for the measure of mask-induced line-edge roughness in extreme ultraviolet lithography," Appl. Opt. **48**, 3302-3307 (2009).
14. Michael Goldstein, Russ Hudyma, Patrick Naulleau, Stefan Wurm, "Extreme-ultraviolet Microexposure Tool at 0.5 NA for Sub-16 nm Lithography," Opt. Lett. **33**, 2995-2997 (2008).